

Light transport in two-layer tissues

Arnold D. Kim

University of California, Merced
School of Natural Sciences
P.O. Box 2039
Merced, California 95344
E-mail: adkim@ucmerced.edu

Miguel Moscoso

Universidad Carlos III de Madrid
Escuela Politécnica Superior
Grupo de Modelización y Simulación Numérica
Avenida de la Universidad 30
28911 Leganés, Spain
E-mail: moscoso@math.uc3m.es

Abstract. We study theoretically light backscattered by tissues using the radiative transport equation. In particular we consider a two-layered medium in which a finite slab is situated on top of a half space. We solve the one-dimensional problem in which a plane wave is incident normally on the top layer and is the only source of light. The solution to this problem is obtained formally by imposing continuity between the solutions for the upper and lower layers. However, we are interested solely in probing the top layer. Assuming that the optical properties in the lower layer are known, we remove it from the problem yielding a finite slab problem by prescribing an alternate boundary condition. This boundary condition is derived using the theory of Green's functions and is exact. Hence, one needs only to solve the transport equation in a finite slab using this alternate boundary condition. We derive an asymptotic solution for the case when the slab is optically thin. We extend these results to the three-dimensional problem using Fourier transforms. These results are validated by comparisons with numerical solutions for the entire two-layered problem.

© 2005 Society of Photo-Optical Instrumentation Engineers. [DOI: 10.1117/1.1925227]

Keywords: radiative transport equation; backscattering; layered media; Green's function.

Paper 04171RR received Aug. 30, 2004; revised manuscript received Jan. 24, 2005; accepted for publication Feb. 1, 2005; published online Jun. 1, 2005.

1 Introduction

Light propagation in tissues is governed by the theory of radiative transport.¹ The radiative transport equation takes into account absorption and scattering due to inhomogeneities in tissues. Analytical solutions to this integrodifferential equation are known only for relatively simple problems.^{2,3}

For light that has propagated deeply into an optically thick medium, the radiance becomes nearly isotropic due to multiple scattering. For that case the transport equation can be replaced by the diffusion equation.¹ Solving the diffusion equation is much easier than solving the transport equation. However, the diffusion approximation is limited to situations in which the direction dependence of the radiance is nearly negligible. Hence, it does not approximate well the solution to the transport equation near collimated sources and interfaces with significant refractive index mismatch.⁴

The limitations of the diffusion approximation are problematic. Diagnostic measurements at small source-detector separations yield valuable site-specific information that is not available at larger separations.⁵ Moreover, noninvasive measurements are made at the boundary of a medium where the refractive index may be significantly different from that inside the medium. Nonetheless, it is used extensively to model diagnostic data.

Recently, there has been much progress in acquiring diverse sets of diagnostic measurements of spatial, spectral, angular, and polarization variations of light scattered by tissues.⁶

Those data show that these diverse diagnostic measurements are rich with physiological information. However, this information content is not understood well enough that this diversity can be leveraged as a gain in biomedical applications. Modeling this data accurately necessitates a more sophisticated theory than the diffusion approximation. To overcome the limitations inherent to the diffusion approximation, we seek a method to solve the transport equation.

Typically, one solves the transport equation using Monte Carlo simulations. Monte Carlo simulations trace individual photons as they propagate in and interact with the medium. Statistical averages of data collected from following a large number of these photons yield desired results. Although this method gives exact results up to statistical errors, the convergence rate is $O(N^{1/2})$ with N denoting the number of collected photons. This slow convergence rate motivates us to seek a direct numerical solution method as an alternative.

A two-layered medium is a useful model for tissues because it allows for different optical properties to be prescribed for the superficial and deep regions of tissues. For example, this difference between optical properties is necessary to model accurately light propagation through tissues consisting of epithelial and stromal tissue layers. Because most cancers originate in the epithelial layer,^{6,7} it is important to determine how light has interacted with this layer. However, light also penetrates into the stromal layer, multiply scatters within it, and interacts back and forth with the epithelial layer before emerging at the surface. The coupling between these two lay-

Address all correspondence to A. D. Kim, School of Natural Sciences, University of California, Merced, P.O. Box 2039, Merced, California 95344. Tel: 209.724.2951; Fax: 209.724.2912; E-mail: adkim@ucmerced.edu.

ers is nontrivial since photons can scatter between them any number of times.

There are several studies that have used the diffusion approximation to calculate the reflectance due to a two-layer medium.^{8–12} Because the diffusion approximation is not accurate for describing light near sources, its use in the top layer can be problematic. A recent study by Chang et al.¹³ has proposed using the Beer–Lambert law for the epithelial tissue layer and the diffusion approximation in the stromal layer. Alternatively, hybrid methods that solve the transport equation in the top layer using Monte Carlo simulations and solve the diffusion approximation in the bottom one have been used to study this problem.^{14,15} These methods overcome the limitations of the diffusion approximation. However, both of them use heuristic arguments, and are not derived systematically from the transport equation. Rather, they have been shown empirically to agree with the solution of the transport equation.

From the experimental point of view, different gating techniques have been proposed to discriminate between the light coming from the superficial and deep tissue layers. Time gating¹⁶ uses picosecond time-resolved techniques to select the signal arriving early to the detector thereby excluding the multiply scattered photons that have penetrated deeply. Polarization gating^{17,18} is based on the fact that single scattering in the top layer retains the polarization state of the incident light, while the degree of polarization of multiply scattered light in the deep tissue is nearly negligible. Therefore, the information contained in backscattered light from epithelial tissues is almost completely contained in the photons that retain their original polarization state.

Even though these sophisticated experimental techniques can be used to study epithelial tissue layers, the need to analyze, interpret, and predict diverse data from diagnostic measurements accurately necessitates the development of sophisticated models. We address this need by solving the transport equation. Since we shall use a direct numerical solution method, it is more complicated mathematically than solving the problem using the diffusion equation or Monte Carlo simulations. However, a direct numerical solution method provides a tool to investigate the information content available in diverse diagnostic data.

In this paper we shall study the scalar, steady-state transport equation. In particular, we shall calculate the solution of the transport equation for a two-layered medium in which a finite slab resides on top of a half space. Using the theory of Green’s functions, we replace the two-layer problem by an equivalent slab problem. The key to this equivalent slab problem is the prescription of an alternate boundary condition at the bottom of the slab that takes into account exactly the multiple scattering of light in the lower layer. This boundary condition is given in terms of the surface Green’s function for the half space. The surface Green’s function is related directly to the volume Green’s function. We use the method due to Kim¹⁹ to compute the volume Green’s function for the half space. By solving this equivalent slab problem rather than the two-layer problem, we reduce the computational domain to the top layer. Hence, this result is useful for developing methods to probe epithelial tissue layers.

For the case in which the finite slab is optically thin, we compute an asymptotic solution to the equivalent slab prob-

lem. This analytical solution gives a systematic representation of interaction between the top and bottom layer. We shall show that this thin layer approximation works well for all angles except those that are near-grazing.

The paper is organized as follows. In Sec. 2 we discuss the two-layer problem and its direct numerical solution in one spatial dimension. In Sec. 3 we discuss the equivalent problem in the top slab using the alternate boundary condition at the bottom of the slab. Included in this discussion is the computation of the surface Green’s function for the lower medium and the direct numerical solution of the problem. In Sec. 4 we compute an asymptotic approximation to the equivalent slab problem for the case in which the slab is optically thin. In Sec. 5 we discuss the extension of this work to three-dimensional problems. Section 6 contains numerical results demonstrating the validity of this theory. Section 7 is the conclusions. The Appendix gives the method used to calculate plane wave solutions that are used throughout this discussion.

2 The Two-Layer Problem

The radiance Ψ is the radiant power per unit solid angle per unit area perpendicular to the direction of propagation. It depends on the unit direction vector $\boldsymbol{\omega}$ and the position vector \mathbf{r} . The radiance in tissues is governed by the transport equation

$$\boldsymbol{\omega} \cdot \nabla \Psi + \mu_a \Psi = -\mu_s \Psi + \mu_s \int_{\Omega} f(\boldsymbol{\omega} \cdot \boldsymbol{\omega}') \Psi(\boldsymbol{\omega}', \mathbf{r}) d\boldsymbol{\omega}'. \quad (1)$$

Here, μ_a and μ_s denote the absorbing and scattering coefficients, respectively. Integration is taken over the unit sphere Ω . The scattering phase function f gives the fraction of light scattered in direction $\boldsymbol{\omega}$ due to light incident in direction $\boldsymbol{\omega}'$. The unit direction vector $\boldsymbol{\omega}$ is given in terms of the cosine of the polar angle $\nu = \cos \theta$ and the azimuthal angle φ . We assume here that the scattering phase function f depends only on $\boldsymbol{\omega} \cdot \boldsymbol{\omega}'$. It is normalized according to

$$2\pi \int_{-1}^1 f(\boldsymbol{\omega} \cdot \boldsymbol{\omega}') d(\boldsymbol{\omega} \cdot \boldsymbol{\omega}') = 1. \quad (2)$$

We seek the solution of (1) in a two-layered medium in which a finite slab $0 < z < z_0$ is situated on top of the half space $z > z_0$. In particular, we wish to calculate the light backscattered by this medium. The optical properties: the absorption coefficient μ_a , the scattering coefficient μ_s , and the scattering phase function f , are homogeneous in each layer. However, the properties in one layer may be different from the other layer. To acknowledge this difference, we denote the optical properties in the top layer by $(\mu_{a1}, \mu_{s1}, f_1)$, and those in the lower layer by $(\mu_{a2}, \mu_{s2}, f_2)$. For simplicity, we assume index-matched boundaries. This discussion extends readily for the case in which boundaries are index mismatched.²⁰

2.1 The One-Dimensional Problem

To begin this discussion, we study the one-dimensional problem. For this problem, a plane wave that illuminates normal to the top boundary of the slab is the only source. A sketch of this problem is shown in Fig. 1.

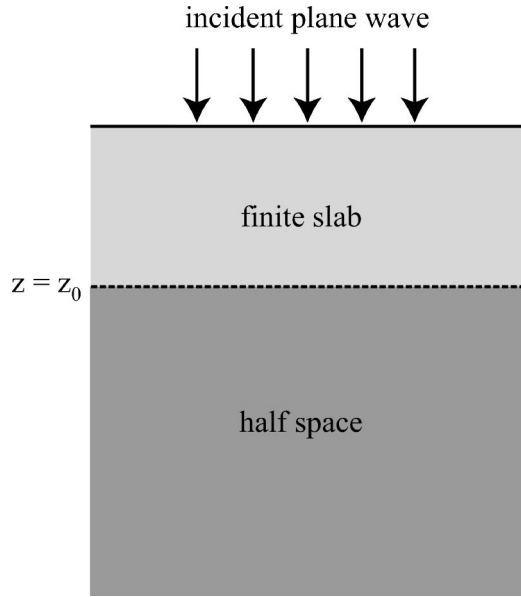


Fig. 1 A sketch of the two-layer problem.

For this problem the solution Ψ is independent of the transverse spatial coordinates x and y . In addition, because we consider a plane wave incident normally on the medium, the solution is axisymmetric and hence, independent of φ . We represent the solution Ψ of this one dimensional, two-layer problem as

$$\Psi(\nu, z) = \begin{cases} \Psi_1(\nu, z), & 0 < z < z_0, \\ \Psi_2(\nu, z), & z > z_0, \end{cases} \quad (3)$$

with Ψ_1 satisfying

$$\begin{aligned} \nu \partial_z \Psi_1 + \mu_{a1} \Psi_1 = & -\mu_{s1} \Psi_1 + \mu_{s1} \int_{-1}^1 p_1(\nu, \nu') \\ & \times \Psi_1(\nu', z) d\nu', \quad 0 < z < z_0, \end{aligned} \quad (4)$$

and Ψ_2 satisfying

$$\begin{aligned} \nu \partial_z \Psi_2 + \mu_{a2} \Psi_2 = & -\mu_{s2} \Psi_2 + \mu_{s2} \int_{-1}^1 p_2(\nu, \nu') \\ & \times \Psi_2(\nu', z) d\nu', \quad z > z_0. \end{aligned} \quad (5)$$

The functions $p_{1,2}$ are related to $f_{1,2}$ by

$$\begin{aligned} p_{1,2}(\nu, \nu') = & \int_{-\pi}^{\pi} f_{1,2}[\nu \nu' + \sqrt{(1-\nu^2)(1-\nu'^2)} \\ & \times \cos(\varphi - \varphi')] d(\varphi - \varphi'). \end{aligned} \quad (6)$$

At $z=0$ we prescribe the boundary condition

$$\Psi_1(\nu, 0) = \frac{F}{2\pi} \delta(\nu - 1), \quad 0 < \nu \leq 1. \quad (7)$$

This boundary condition corresponds to a plane wave with flux F incident normally on the boundary at $z=0$. At the interface located at $z=z_0$, we prescribe that the radiance must be continuous over all directions

$$\Psi_1(\nu, z_0) = \Psi_2(\nu, z_0), \quad -1 \leq \nu \leq 1. \quad (8)$$

In addition, we prescribe that $\Psi_2 \rightarrow 0$ as $z \rightarrow \infty$.

2.2 The Direct Numerical Solution Method

We discuss a direct solution method to solve (4) and (5) subject to (7) and (8). This method makes use of plane wave solutions to the transport equation. Plane wave solutions are solutions of the form $\Psi(\nu, z) = e^{\lambda z} V(\nu)$. After substituting this solution form into the transport equations and discretizing the cosine of the polar angle ν , we obtain a $M \times M$ eigenvalue problem for each layer with M denoting the number of discrete angles we use (see the Appendix). For the numerically calculated plane wave solutions corresponding to the medium with the optical properties of the upper layer, we denote the eigenvalues by λ_j and the eigenvectors by $V_j(\nu_m)$. For the plane wave solutions corresponding to the medium with optical properties of the lower layer, we denote the eigenvalues by ξ_j and the eigenvectors by $W_j(\nu_m)$. Using these two sets of plane wave solutions, we seek Ψ_1 in the form

$$\begin{aligned} \Psi_1(\nu_m, z) = & \sum_{j=1}^{M/2} [a_j V_j(-\nu_m) e^{-\lambda_j z} \\ & + b_j V_j(\nu_m) e^{\lambda_j(z-z_0)}], \quad m = 1, \dots, M. \end{aligned} \quad (9)$$

Here, we have used the symmetry property of plane wave modes in which $\lambda_{-j} = -\lambda_j$ and $V_{-j}(\nu) = V_j(-\nu)$. Similarly, we seek Ψ_2 in the form

$$\Psi_2(\nu_m, z) = \sum_{j=1}^{M/2} c_j W_j(-\nu_m) e^{-\xi_j(z-z_0)}, \quad m = 1, \dots, M. \quad (10)$$

The form for Ψ_2 given in (10) satisfies the condition that $\Psi_2 \rightarrow 0$ as $z \rightarrow \infty$.

It remains to determine the expansion coefficients a_j , b_j , and c_j comprising $3M/2$ unknowns. We do this by substituting (9) and (10) into boundary conditions (7) and (8). By substituting (9) into (7), we obtain

$$\begin{aligned} & \sum_{j=1}^{M/2} [a_j V_j(-\nu_m) + b_j V_j(\nu_m) e^{-\lambda_j z_0}] \\ & = \frac{F}{2\pi} s(\nu_m), \quad m = M/2 + 1, \dots, M. \end{aligned} \quad (11)$$

In (11) we have replaced $\delta(\nu-1)$ in (7) by a narrow Gaussian centered about $\nu=1$ denoted by $s(\nu)$. By substituting (9) and (10) into (8), we obtain

$$\sum_{j=1}^{M/2} [a_j V_j(-\nu_m) e^{-\lambda_j z_0} + b_j V_j(\nu_m) - c_j W_j(-\nu_m)] = 0, \quad m = 1, \dots, M. \quad (12)$$

Equations (11) and (12) comprise a $3M/2 \times 3M/2$ linear system of equations. After solution of this system, we compute the radiance backscattered by evaluating

$$\Psi_1(\nu_m, 0) = \sum_{j=1}^{M/2} [a_j V_j(-\nu_m) + b_j V_j(\nu_m) e^{-\lambda_j z_0}], \quad m = 1, \dots, M/2. \quad (13)$$

3 The Equivalent Problem in the Slab

To compute the solution to the two-layer problem, one must solve two transport equations for the slab and for the half space. Those two solutions must satisfy the matching condition at $z=z_0$ given by (8). Because most early precancerous tissues develop in the epithelial layer, we would like to focus our analysis on the top layer. However, diagnostic measurements taken at the boundary $z=0$ include light that has penetrated through the top layer into the bottom one, and scattered from there up into the slab. From there, light scatters back and forth between the two layers any number of times before emerging as backscattered light. This interaction is taken into account by the coupling of Ψ_1 and Ψ_2 in (8).

Suppose that the optical properties of the bottom layer are known. Under this assumption, we introduce a boundary condition at $z=z_0$ that takes into account light backscattered by the bottom layer. In this way we are able to replace the two-layer problem by an equivalent problem for a slab corresponding to the top layer.

Consider the half space problem in which the top layer has been removed. A light source $\Psi(\nu, z_0)$ for $0 < \nu \leq 1$ is incident on the half space at the boundary $z=z_0$. There are no other sources. The radiance backscattered by this half space is given in terms of the surface Green's function G_s as³

$$\Psi(\nu, z_0) = \int_0^1 G_s(\nu, \nu') \Psi(\nu', z_0) d\nu', \quad -1 \leq \nu < 0. \quad (14)$$

Equation (14) asserts that the radiance backscattered is given by the superposition of the surface Green's function with the source incident on the boundary. The surface Green's function is written in terms of the volume Green's function G as³

$$G_s(\nu; \nu') = \nu' G(\nu, z_0^-; \nu', z_0^+). \quad (15)$$

Here, G is evaluated just outside the half space ($z=z_0^-$) for a source evaluated just inside the half space ($z=z_0^+$).

Equation (14) gives the radiance backscattered by the lower medium due to light incident from above it. We can interpret this formula as a diffuse reflection law (see Fig. 2). Rather than solve the problem in the lower layer, we can use

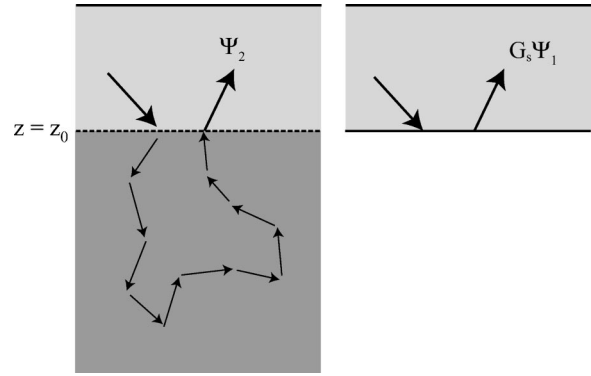


Fig. 2 A sketch of the equivalent slab problem in which we replace the transport equation in the lower half space by an alternate boundary condition given in terms of the surface Green's function G_s .

(14) as a boundary condition for Ψ_1 at $z=z_0$ and for $-1 \leq \nu < 0$. Hence, we replace the original two-layer problem by one in the finite slab $0 < z < z_0$:

$$\nu \partial_z \Psi_1 + \mu_{a1} \Psi_1 = -\mu_{s1} \Psi_1 + \mu_{s1} \int_{-1}^1 p_1(\nu, \nu') \times \Psi_1(\nu', z) d\nu', \quad 0 < z < z_0, \quad (16)$$

subject to

$$\Psi_1(\nu, 0) = \frac{F}{2\pi} \delta(\nu-1), \quad 0 < \nu \leq 1, \quad (17)$$

and

$$\Psi_1(\nu, z_0) = \int_0^1 G_s(\nu; \nu') \Psi_1(\nu', z_0) d\nu', \quad -1 \leq \nu < 0. \quad (18)$$

The boundary condition given by (18) can be written formally also in terms of the Chandrasekhar's scattering S function.² For the case that scattering is isotropic, this boundary condition can be written in closed-form in terms of Chandrasekhar's H -function² or using the Green's function given by Case and Zweifel.³

3.1 Computing the Surface Green's Function

The key to the equivalent slab problem given by (16) subject to (17) and (18) is the surface Green's function $G_s(\nu; \nu')$. We use plane wave solutions to compute the Green's function. We use the same notation for plane wave solutions that we used above in Sec. 2.2. Using those plane wave solutions, the surface Green's function is given by¹⁹

$$G_s(\nu_m; \nu_{m'}) = \sum_{j=1}^{M/2} \left[W_j(\nu_m) W_j(\nu_{m'}) \nu_{m'} - W_j(-\nu_m) \sum_{k=1}^{M/2} Y_{jk} W_k(\nu_{m'}) \nu_{m'} \right], \quad m = 1, \dots, M/2, \quad m' = M/2 + 1, \dots, M. \quad (19)$$

The coefficients Y_{jk} are the solution to the linear system

$$\sum_{j=1}^{M/2} W_j(-\nu_m) Y_{jk} = W_k(\nu_m), \quad m = M/2 + 1, \dots, M, \quad (20)$$

$$k = 1, \dots, M/2.$$

Because the optical properties of the lower layer are assumed to be known, we can precompute the plane wave solutions for that medium using the method described in the Appendix.

3.2 The Direct Numerical Solution Method

To solve the equivalent slab problem, we seek Ψ_1 in the same form given in (9). Hence, it remains to determine the expansion coefficients a_j and b_j comprising M unknowns. We determine these unknowns by substituting (9) into the boundary conditions (17) and (18). Equation (17) is exactly the same as (7), so we still impose (11). Substituting (9) into (18) and replacing the integral by the Gauss–Legendre quadrature rule used to calculate the plane wave solutions, we obtain

$$\sum_{j=1}^{M/2} \left\{ a_j e^{-\lambda_j z_0} \left[V_j(-\nu_m) - \sum_{m'=M/2+1}^M G_s(\nu_m; \nu_{m'}) \right. \right. \\ \left. \left. \times V_j(-\nu_{m'}) w_{m'} \right] \right\} + \sum_{j=1}^{M/2} \left\{ b_j \left[V_j(\nu_m) \right. \right. \\ \left. \left. - \sum_{m'=M/2+1}^M G_s(\nu_m; \nu_{m'}) V_j(\nu_{m'}) w_{m'} \right] \right\} = 0, \quad (21)$$

$$m = 1, \dots, M/2.$$

Hence, (11) and (21) comprise a $M \times M$ linear system of equations. After solution of this system, we compute the radiance backscattered using (13) as was done for the two-layer problem.

The equivalent slab problem offers some savings in computational complexity. Instead of solving the $3M/2 \times 3M/2$ linear system given by (11) and (12), we only have to solve an $M \times M$ system given by (11) and (21). However, we still have to solve two $M \times M$ eigenvalue problems for the plane wave solutions. This is the main source of work in solving the two-layer problem. However, when the optical properties of the lower layer are known, the plane wave solutions for the lower layer can be calculated beforehand and stored in physical memory for later use. This is the case, for example, when one is interested on retrieving only the optical properties of the top layer where most precancers form. The computational savings from precalculating the plane wave solutions for the lower layer are more significant for three-dimensional problems, since they include the φ dependence in the angle discretization.

4 Thin Layer Approximation

Suppose the top layer is very thin compared with the scattering mean free path $z_0 \ll l_s = 1/\mu_s$. Then, we can compute an analytical approximation to the solution of the equivalent slab problem. We introduce the nondimensional variables

$$\epsilon = \mu_{s1} z_0, \quad (22a)$$

$$\alpha = \mu_{a1} z_0, \quad (22b)$$

$$\bar{z} = z/z_0. \quad (22c)$$

In terms of these nondimensional variables, the slab problem is

$$\nu \partial_{\bar{z}} \Psi + \alpha \Psi = \epsilon L \Psi, \quad 0 < \bar{z} < 1, \quad (23a)$$

$$\Psi(\nu, 0) = \frac{F}{2\pi} \delta(\nu - 1), \quad 0 < \nu \leq 1, \quad (23b)$$

$$\Psi(\nu, 1) = \int_0^1 G_s(\nu, \nu') \Psi(\nu', 1) d\nu', \quad -1 \leq \nu < 0. \quad (23c)$$

Here, we have introduced the operator L defined as

$$L \Psi = -\Psi + \int_{-1}^1 p_1(\nu, \nu') \Psi(\nu', \bar{z}) d\nu'. \quad (24)$$

The thin layer approximation corresponds to the limit in which $\epsilon \rightarrow 0$. In addition, we assume here that α is much smaller than ϵ . This assumption is not necessary, but simplifies the following analysis. Furthermore, it is consistent with typical optical properties for tissues (e.g., the absorption coefficient is approximately one order of magnitude smaller than the scattering coefficient).

We represent Ψ as the asymptotic expansion

$$\Psi(\nu, \bar{z}) \sim \sum_{n=0}^{\infty} \epsilon^n \Psi_n(\nu, \bar{z}). \quad (25)$$

Each term in the series above is determined by substitution of (25) into (23) and matching powers of ϵ .²¹ To $O(1)$ we obtain

$$\nu \partial_{\bar{z}} \Psi_0 = 0, \quad 0 < \bar{z} < 1, \quad (26a)$$

$$\Psi_0(\nu, 0) = \frac{F}{2\pi} \delta(\nu - 1) \quad 0 < \nu \leq 1, \quad (26b)$$

$$\Psi_0(\nu, 1) = \int_0^1 G_s(\nu, \nu') \Psi_0(\nu', 1) d\nu', \quad -1 \leq \nu < 0. \quad (26c)$$

The general solution to (26a) is $\Psi_0 = A(\nu)$. By imposing (26b) we determine that

$$A(\nu) = \frac{F}{2\pi} \delta(\nu - 1), \quad 0 < \nu \leq 1. \quad (27)$$

Substituting (27) into (26c), we obtain

$$A(\nu) = \int_0^1 G_s(\nu, \nu') A(\nu') d\nu' \\ = \int_0^1 G_s(\nu, \nu') \frac{F}{2\pi} \delta(\nu' - 1) d\nu' \quad (28)$$

$$= \frac{F}{2\pi} G_s(\nu, 1), \quad -1 \leq \nu < 0.$$

Hence, the radiance to $O(1)$ is

$$\Psi_0 = A(\nu) = \frac{F}{2\pi} \times \begin{cases} \delta(\nu-1), & 0 < \nu \leq 1, \\ G_s(\nu, 1), & -1 \leq \nu < 0. \end{cases} \quad (29)$$

Because the effects of scattering and absorption do not appear at this order, we observe that Ψ_0 is the response to the two-layer medium as if the top layer were not there. Franceschini et al.²² showed experimentally that the role of the top layer on the reflectance of a two-layer medium is not significant if it is less than ~ 4 mm thick. Here, we have shown that this result follows readily from this systematic treatment of the transport equation.

To $O(\epsilon)$ we obtain

$$\nu \partial_{\bar{z}} \Psi_1 = L \Psi_0, \quad 0 < \bar{z} < 1, \quad (30a)$$

$$\Psi_1(\nu, 0) = 0, \quad 0 < \nu \leq 1, \quad (30b)$$

$$\Psi_1(\nu, 1) = \int_0^1 G_s(\nu, \nu') \Psi_1(\nu', 1) d\nu', \quad -1 \leq \nu < 0. \quad (30c)$$

Substituting (29) into (24), we obtain

$$\begin{aligned} L \Psi_0 &= -A(\nu) + \int_{-1}^1 p_1(\nu, \nu') A(\nu') d\nu' \\ &= -A(\nu) + \frac{F}{2\pi} \int_{-1}^0 p_1(\nu, \nu') G_s(\nu', 1) d\nu' \\ &\quad + \frac{F}{2\pi} \int_0^1 p_1(\nu, \nu') \delta(\nu' - 1) d\nu' \\ &= -A(\nu) + \frac{F}{2\pi} \int_{-1}^0 p_1(\nu, \nu') G_s(\nu', 1) d\nu' \\ &\quad + \frac{F}{2\pi} p_1(\nu, 1) \equiv B(\nu). \end{aligned} \quad (31)$$

The general solution to (30a) is given by $\Psi_1 = B(\nu) \bar{z} / \nu + C(\nu)$. Imposing (30b), we find that

$$C(\nu) = 0, \quad 0 < \nu \leq 1. \quad (32)$$

Imposing (30c) and using (32), we obtain

$$\begin{aligned} C(\nu) &= -\frac{1}{\nu} B(\nu) + \int_0^1 G_s(\nu, \nu') B(\nu') \frac{1}{\nu'} d\nu', \\ &\quad -1 \leq \nu < 0. \end{aligned} \quad (33)$$

Substituting (27) and (31) into integral term in (33), we find that

$$\begin{aligned} C(\nu) &= -\frac{1}{\nu} B(\nu) - \frac{F}{2\pi} G_s(\nu, 1) \\ &\quad + \frac{F}{2\pi} \int_0^1 G_s(\nu, \nu') p_1(\nu', 1) \frac{1}{\nu'} d\nu' \\ &\quad + \frac{F}{2\pi} \int_0^1 G_s(\nu, \nu') \int_{-1}^0 p_1(\nu', \nu'') G_s(\nu'', 1) \\ &\quad \times d\nu'' \frac{1}{\nu'} d\nu', \quad -1 \leq \nu < 0. \end{aligned} \quad (34)$$

Hence, to $O(\epsilon)$ the radiance backscattered by the two-layer medium is

$$\begin{aligned} \Psi(\nu, 0) &\sim \Psi_0(\nu) + \epsilon \Psi_1(\nu, 0), \quad -1 \leq \nu < 0, \\ &= \frac{F}{2\pi} G_s(\nu, 1) \left[1 - \epsilon \left(1 - \frac{1}{\nu} \right) \right] - \epsilon \frac{F}{2\pi \nu} p_1(\nu, 1) \\ &\quad - \epsilon \frac{F}{2\pi \nu} \int_{-1}^0 p_1(\nu, \nu') G_s(\nu', 1) d\nu' \\ &\quad + \epsilon \frac{F}{2\pi} \int_0^1 G_s(\nu, \nu') p_1(\nu', 1) \frac{1}{\nu'} d\nu' \\ &\quad + \epsilon \frac{F}{2\pi} \int_0^1 G_s(\nu, \nu') \int_{-1}^0 p_1(\nu', \nu'') G_s(\nu'', 1) \\ &\quad \times d\nu'' \frac{1}{\nu'} d\nu', \quad -1 \leq \nu < 0. \end{aligned} \quad (35)$$

One can continue this computation in a similar manner to obtain higher order corrections. For example, one can consider the limit in which $\alpha = O(\epsilon^2)$. Hence, by computing the asymptotic expansion of Ψ up to $O(\epsilon^2)$, one takes into account absorption in the top layer. This computation involves only a sequence of elementary calculations. However, the analytical expressions become complicated, so we do not discuss them here.

The thin layer approximation yields a power series in \bar{z} . This power series is related to the successive scattering or Neumann series. For that case the leading order term in that series is given by the Beer–Lambert law.¹ Hence, it is proportional to an exponential function decaying with respect to depth. Consequently, higher order corrections involve exponential functions also. By expanding these exponential functions as Taylor series and truncating them in a manner that is consistent with the balance of scales given in (22), we can show that the thin layer approximation and the successive order scattering series are equivalent asymptotically. Hence, we have shown that the model due to Chang et al.¹³ in which they use the Beer–Lambert law for the top layer follows readily from this systematic treatment of the transport equation. Moreover, this perturbation analysis provides an estimate for the error incurred by applying this approximation. Hence, this analysis provides additional insight into the range of validity of that model.

5 Extension to Three-Dimensional Problems

Even though we have discussed and demonstrated this theory for the one-dimensional problem, it extends easily to the three-dimensional problem. For that case the equivalent slab problem is

$$\begin{aligned} & \nu \partial_z \Psi + \sqrt{1 - \nu^2} (\cos \varphi \partial_x \Psi + \sin \varphi \partial_y \Psi) + \mu_{a1} \Psi \\ &= -\mu_{s1} \Psi + \mu_{s1} \int_{-\pi}^{\pi} \int_{-1}^1 f_1(\nu, \nu', \varphi - \varphi') \\ & \quad \times \Psi(\nu', \varphi', x, y, z) d\nu' d\varphi', \quad 0 < z < z_0, \end{aligned} \quad (36)$$

with the following boundary condition at $z = 0$:

$$\begin{aligned} \Psi(\nu, \varphi, x, y, 0) &= F(x, y) \delta(\nu - \nu_0) \delta(\varphi - \varphi_0), \\ & 0 < \nu \leq 1, \quad -\pi \leq \varphi < \pi, \end{aligned} \quad (37)$$

and the following boundary condition at $z = z_0$:

$$\begin{aligned} & \Psi(\nu, \varphi, x, y, z_0) \\ &= \int_{-\infty}^{\infty} \int_{-\infty}^{\infty} \int_{-\pi}^{\pi} \int_0^1 G_s(\nu, \varphi, \nu', \varphi', x - x', y - y', z_0) \\ & \quad \times \Psi(\nu', \varphi', x', y') d\nu' d\varphi' dx' dy', \\ & -1 \leq \nu < 0, \quad -\pi \leq \varphi < \pi, \quad -\infty < x, y < \infty. \end{aligned} \quad (38)$$

Equation (37) corresponds to light incident on the boundary at $z = 0$ with transverse spatial distribution $F(x, y)$ in direction (ν_0, φ_0) . Equation (38) is a nonlocal boundary condition since it involves integration over all x and y .

Rather than solve the slab problem in the physical domain, we solve for its Fourier transform with respect to the transverse spatial coordinates, x and y . The Fourier transform of Ψ with respect to x and y is

$$\begin{aligned} \hat{\Psi}(\nu, \varphi, z; k_x, k_y) &= \frac{1}{(2\pi)^2} \int_{-\infty}^{\infty} \int_{-\infty}^{\infty} \Psi(\nu, \varphi, x, y, z) \\ & \quad \times e^{-ik_x x - ik_y y} dx dy. \end{aligned} \quad (39)$$

Fourier transforming (36) we obtain

$$\begin{aligned} & \nu \partial_z \hat{\Psi} + i\sqrt{1 - \nu^2} (k_x \cos \varphi + k_y \sin \varphi) \hat{\Psi} + \mu_{a1} \hat{\Psi} \\ &= -\mu_{s1} \hat{\Psi} + \mu_{s1} \int_{-\pi}^{\pi} \int_{-1}^1 f_1(\nu, \nu', \varphi - \varphi') \\ & \quad \times \hat{\Psi}(\nu', \varphi', z; k_x, k_y) d\nu' d\varphi', \quad 0 < z < z_0. \end{aligned} \quad (40)$$

Fourier transforming (37) yields

$$\begin{aligned} \hat{\Psi}(\nu, \varphi, z; k_x, k_y) &= \hat{F}(k_x, k_y) \delta(\nu - \nu_0) \delta(\varphi - \varphi_0), \\ & 0 < \nu \leq 1, \quad -\pi \leq \varphi < \pi, \end{aligned} \quad (41)$$

with \hat{F} the Fourier transform of F . The integrals in (38) with respect to x' and y' comprise a two-dimensional Fourier convolution. Hence, Fourier transforming (38) yields

$$\begin{aligned} & \hat{\Psi}(\nu, \varphi, z_0; k_x, k_y) \\ &= \int_{-\pi}^{\pi} \int_0^1 \hat{G}_s(\nu, \varphi, \nu', \varphi'; k_x, k_y) \hat{\Psi}(\nu', \varphi', z_0; k_x, k_y) \\ & \quad \times d\nu' d\varphi', \quad -1 \leq \nu < 0, \quad -\pi \leq \varphi < \pi. \end{aligned} \quad (42)$$

In contrast to (38), the boundary condition given by (42) is local since it depends on (k_x, k_y) parametrically only.

Kim¹⁶ gives a method to compute the volume Green's function for the half space in this Fourier domain. Using that result we compute \hat{G}_s . Hence, we are able to solve the equivalent slab problem for each transverse spatial frequency pair (k_x, k_y) over a discrete spectrum. In fact, the equivalent slab problem for each (k_x, k_y) pair is a one-dimensional problem just like the one we have discussed earlier. Once that spectrum is computed, we recover the solution in the physical domain using discrete inverse Fourier transforms. Because the slab problem for each spatial frequency pair is decoupled from the others, this computation is easily implemented on a concurrent computing system thereby increasing the efficiency of this calculation.

6 Numerical Results

We have used the Henyey–Greenstein scattering phase function to compute our numerical solutions. It is given by

$$f(\omega \cdot \omega') = \frac{1}{4\pi} \frac{1 - g^2}{(1 + g^2 - 2g\omega \cdot \omega')^{3/2}}. \quad (43)$$

Its only parameter is the anisotropy factor g . By computing (6) using (43), we determine the corresponding scattering function in the one-dimensional problem to be

$$p(\nu, \nu') = \frac{2(1 - g^2)}{\pi(a - b)\sqrt{a + b}} E\left(\frac{2b}{a + b}\right). \quad (44)$$

Here, $a = 1 + g^2 + 2g\nu\nu'$, $b = 2g\sqrt{(1 - \nu^2)(1 - \nu'^2)}$ and $E(k)$ is the complete elliptic integral of the second kind.

For the top layer, we have set the absorption coefficient to be $\mu_{a1} = 0.02 \text{ mm}^{-1}$ and the scattering coefficient to be $\mu_{s1} = 6.50 \text{ mm}^{-1}$. For the bottom layer, we have set the absorption coefficient to be $\mu_{a1} = 0.01 \text{ mm}^{-1}$ and the scattering coefficient to be $\mu_{s1} = 6.00 \text{ mm}^{-1}$. For both layers, we have set the anisotropy factor to be $g = 0.80$. We have taken these values from the study by Kienle et al.⁹

6.1 Plane Wave Source

In Fig. 3 we show numerical results for the case in which a plane wave is incident normally on the two-layer medium. The plane wave solutions that we calculated numerically used $M = 64$ Gauss–Legendre quadrature points. We show the solutions calculated for the two-layer problem (“x” symbols), the equivalent slab problem (solid curves) and the thin layer approximation (dashed curves). These solutions have been calculated for different top layer thicknesses: (a) $z_0 = 0.1 \text{ mm}$, (b) $z_0 = 0.5 \text{ mm}$, (c) $z_0 = 2.0 \text{ mm}$, and (d) $z_0 = 6.0 \text{ mm}$.

In all of these results we observe that the solutions to the two-layer problem and the equivalent slab problem are indis-

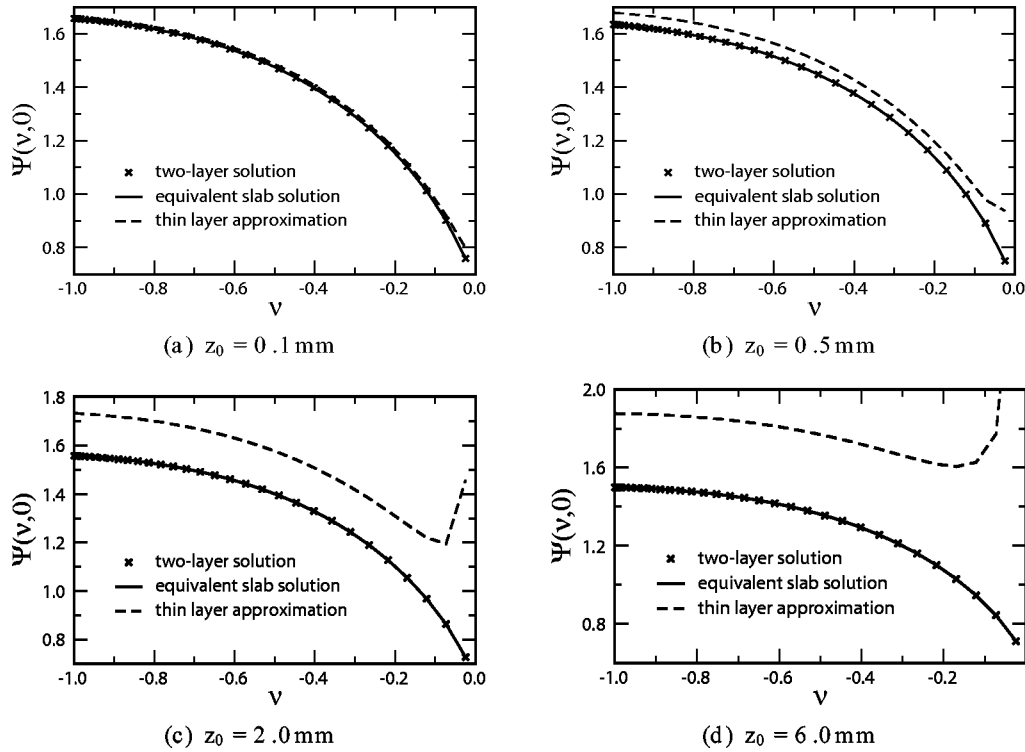


Fig. 3 The radiance backscattered by a two-layer medium due to a plane wave normally incident on the medium. The optical properties of the top slab are $(\mu_{a1}, \mu_{s1}, g_1) = (0.02 \text{ mm}^{-1}, 6.5 \text{ mm}^{-1}, 0.80)$ and the optical properties of the bottom half space are $(\mu_{a2}, \mu_{s2}, g_2) = (0.01 \text{ mm}^{-1}, 6.0 \text{ mm}^{-1}, 0.80)$. The thickness of the top slab is (a) $z_0 = 0.1 \text{ mm}$, (b) $z_0 = 0.5 \text{ mm}$, (c) $z_0 = 2.0 \text{ mm}$, and (d) $z_0 = 6.0 \text{ mm}$. The x symbols are for the solution to the two-layer problem, the solid curve is for the solution of the equivalent slab problem and the dashed curved is the thin layer approximation.

tinguishable. Because the theory underlying the equivalent slab problem is exact, the only quantitative differences between these results are below the double precision arithmetic used to calculate them. The thin layer approximation gives good agreement for $z_0 = 0.1 \text{ mm}$ corresponding to $\epsilon = 0.65$. For the cases with larger slab thicknesses, we observe that the thin layer approximation is not accurate. The accuracy of this approximation breaks down especially for near-grazing angles for which $\nu \approx 0$. This break down occurs because higher order scattering events, which are not taken into account by the thin layer approximation, are significant for near-grazing angles.

6.2 Gaussian Beam Source

Using the extension of the theory discussed in Sec. 5, we have computed the solution of the two-layer problem and the equivalent slab problem due to a Gaussian beam incident normally on the medium. For that case, we can reduce the number of independent variables by working in cylindrical coordinates. Because the beam is incident normally on the medium, the problem is axisymmetric. Hence, the reflectance is defined by the Hankel transform

$$R(\rho) = \frac{1}{2\pi} \int_0^\infty \hat{F}(k) J_0(k\rho) k dk, \quad (45)$$

with

$$\hat{F}(k) = \int_{-\pi}^\pi \int_{-1}^0 \hat{\Psi}(\nu, \varphi, z=0; k) \nu d\nu d\varphi. \quad (46)$$

Here $\rho = (x^2 + y^2)^{1/2}$ and $k = (k_x^2 + k_y^2)^{1/2}$. Additional details on the implementation of the direct numerical solution including the numerical calculation of (45) are contained in Ref. 23.

In Fig. 4 we show the radial dependence of the reflectance due to a Gaussian beam incident normally on the medium. The beam width has been set to 2 mm. The plane wave solutions that we calculated numerically used $M = 16$ for the Gauss product quadrature rule. We show the solutions calculated for the two-layer problem (x symbols) and the equivalent slab problem (solid curves). These solutions have been calculated for different top layer thicknesses: (a) $z_0 = 0.5 \text{ mm}$, (b) $z_0 = 2.0 \text{ mm}$, and (c) $z_0 = 6.0 \text{ mm}$. For all cases we observe that the solutions to the two-layer problem are indistinguishable from those to the equivalent slab problem.

7 Conclusions

We have discussed the direct numerical solution of the transport equation for a two-layer medium. Using the theory of Green's functions, we have also reduced the two-layer problem to an equivalent slab problem. This equivalent slab problem uses an alternate boundary condition given in terms of the surface Green's function for the lower layer. Hence, it depends only on the optical properties of the lower layer. The theory behind the equivalent slab problem is exact.

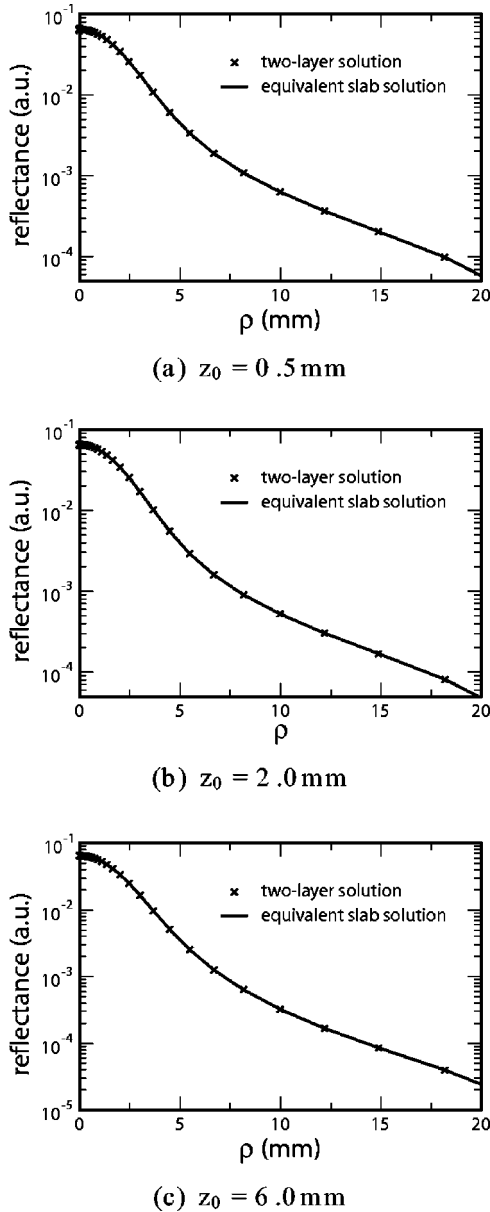


Fig. 4 The reflectance by a two-layer medium due to a Gaussian beam normally incident on the medium. All parameters are the same as for Fig. 3. The beam width is 2.0 mm. The thickness of the top slab is (a) $z_0=0.5$ mm, (b) $z_0=2.0$ mm, and (c) $z_0=6.0$ mm. The x symbols are for the solution to the two-layer problem, and the solid curve is for the solution of the equivalent slab problem.

We have discussed in detail the one-dimensional problem in which a plane wave is incident normally on the top layer. Numerical results confirm that the solutions to the two-layer problem and the equivalent slab problem are equal as expected. This theory extends easily to three-dimensional problems through the use of Fourier transform methods. We have shown numerical results for the problem in which Gaussian beam is incident normally on the medium. Again, the solutions given by the two-layer problem and the equivalent slab problem are indistinguishable.

For the case in which the top layer is optically thin, we have derived an asymptotic approximation. The backscattered

radiance given by the thin layer approximation agrees well with that given by the numerical solution to the two-layer problem. However, this approximation breaks down when the thickness of the top layer increases. Our numerical results confirm this. The accuracy breaks down most dramatically for near-grazing angles. This discrepancy is because backscattered light at near-grazing angles is made up of multiply scattered light that is not taken into account by this asymptotic theory.

These results suggest that this equivalent slab problem should be extremely useful for studying the epithelial tissue layer when the optical properties of the stromal layer are known.

Appendix: Plane Wave Solutions

Plane wave solutions are a general class of solutions that take the form $\Psi(\nu, z) = e^{\lambda z} V(\nu)$. Substituting this solution form into the transport equation yields

$$\lambda \nu V + \mu_a V = -\mu_s V + \mu_s \int_{-1}^1 p(\nu, \nu') V(\nu') d\nu'. \tag{A1}$$

Plane wave solutions have the following three properties.¹⁹

1. For any pair $[\lambda, V(\nu)]$ satisfying (A1), the pair $[-\lambda, V(-\nu)]$, satisfies (A1) also. In light of this symmetry, we order and index the eigenvalues so that $\lambda_j \leq 0$ for $j \leq 0$.
2. The eigenfunctions $V_j(\nu)$ are orthogonal in that they satisfy

$$(\lambda_j - \lambda_k) \int_{-1}^1 V_j(\nu) V_k(\nu) \nu d\nu = 0, \quad j \neq k. \tag{A2}$$

We normalize the plane wave solutions according to

$$\int_{-1}^1 V_j(\nu) V_j(\nu) \nu d\nu = -j/|j|. \tag{A3}$$

The set of eigenfunctions $\{V_j(\nu)\}$ are complete over the full range. Hence, any arbitrary function can be expanded in terms of plane wave solutions.

We cannot calculate the plane wave solutions analytically, in general. Hence, we calculate them numerically using the discrete ordinate method. We approximate the integral operation in (A1) using the Gauss–Legendre quadrature rule

$$\int_{-1}^1 p(\nu, \nu') V(\nu') d\nu' \approx \sum_{m=1}^M p(\nu, \nu_m) V(\nu_m) w_m, \tag{A4}$$

with ν_m and w_m denoting the quadrature abscissas and weights, respectively. Seeking the values of $V(\nu)$ at the quadrature abscissas in (A1) and replacing the integral operation by (A4), we obtain the $M \times M$ eigenvalue problem

$$\begin{aligned} & \lambda \nu_m V(\nu_m) + \mu_a V(\nu_m) \\ & = -\mu_s V(\nu_m) + \mu_s \sum_{m'=1}^M p(\nu_m, \nu_{m'}) V(\nu_{m'}) w_{m'}, \\ & m = 1, \dots, M. \end{aligned} \quad (\text{A5})$$

To normalize the eigenvectors as in (A3), we use the Gauss–Legendre quadrature rule to compute the normalization factor

$$\gamma_j = \sum_{m=1}^M V(\nu_m) V(\nu_m) \nu_m w_m. \quad (\text{A6})$$

Then we scale the calculated eigenvectors by $\sqrt{-\gamma_j}$ for $j > 0$ and by $\sqrt{+\gamma_j}$ for $j < 0$.

Because of the Gauss–Legendre quadrature rule is symmetric about the origin, the numerically calculated plane wave solutions obey the symmetry property. Hence, $\lambda_{-j} = -\lambda_j$ and $V_{-j}(\nu_m) = V_j(-\nu_m) = V_j(\nu_{M-m+1})$ for $j = 1, \dots, M$. We order and index the eigenvalues as

$$\lambda_{-M/2} < \dots < \lambda_{-1} < \lambda_{+1} < \dots < \lambda_{+M/2}. \quad (\text{A7})$$

For the three-dimensional problem given in (40), one must include the φ dependence of the radiance. The method to calculate plane wave solutions follows in a similar way as shown above for the one-dimensional problem. We use a product Gaussian quadrature rule to approximate the integral operations:

$$\begin{aligned} & \int_{-\pi}^{\pi} \int_{-1}^1 p(\nu, \nu', \varphi - \varphi') V(\nu', \varphi') d\nu' d\varphi' \\ & \approx \sum_{n'=1}^{2M} \sum_{m'=1}^M p(\nu_m, \nu_{m'}, \varphi_n - \varphi_{n'}) V(\nu_{m'}, \varphi_{n'}) w_{m'} \Delta\varphi. \end{aligned} \quad (\text{A8})$$

Here, $\varphi_n = (n-1)\Delta\varphi$ with $n = 1, \dots, 2M$ and $\Delta\varphi = \pi/M$. Replacing the integrals in (40) by (A8) and seeking the plane wave solutions at the product quadrature abscissas: $V(\nu_m, \varphi_n)$, we obtain the $2M^2 \times 2M^2$ eigenvalue problem

$$\begin{aligned} & \lambda \nu_m V(\nu_m, \varphi_n) + i\sqrt{1 - \nu_m^2} (k_x \cos \varphi_n + k_y \sin \varphi_n) V(\nu_m, \varphi_n) \\ & + \mu_a V(\nu_m, \varphi_n) \\ & = -\mu_s V(\nu_m, \varphi_n) + \mu_s \sum_{n'=1}^{2M} \sum_{m'=1}^M f(\nu_m, \nu_{m'}, \varphi_n - \varphi_{n'}) \\ & \quad \times V(\nu_{m'}, \varphi_{n'}) w_{m'} \Delta\varphi, \quad m = 1, \dots, M, \\ & n = 1, \dots, 2M. \end{aligned} \quad (\text{A9})$$

References

1. A. Ishimaru, *Wave Propagation and Scattering in Random Media*, IEEE, New York (1996).
2. S. Chandrasekhar, *Radiative Transfer*, Dover, New York (1960).
3. K. M. Case and P. F. Zweifel, *Linear Transport Theory*, Addison-Wesley, Reading, MA (1967).
4. C. K. Hayakawa, B. Y. Hill, J. S. You, F. Bevilacqua, J. Spanier, and V. Venugopalan, "Use of the δ - P_1 approximation for recovery of optical absorption, scattering and asymmetry coefficients in turbid media," *Appl. Opt.* **43**, 4677–4684 (2004).
5. V. Venugopalan, J. S. You, and B. J. Tromberg, "Radiative transport in the diffusion approximation: an extension for highly absorbing media and small source-detector separations," *Phys. Rev. E* **58**, 2395–2407 (1998).
6. Y. L. Kim, Y. Liu, R. K. Wali, H. K. Roy, M. J. Goldberg, A. K. Kromin, K. Chen, and V. Backman, "Simultaneous measurement of angular and spectral properties of light scattering for characterization of tissue microarchitecture in its alteration in early precancer," *IEEE J. Sel. Top. Quantum Electron.* **9**, 243–256 (2003).
7. K. Sokolov, R. A. Drezek, K. Gossage, and R. Richards-Kortum, "Reflectance spectroscopy with polarized light: is it sensitive to cellular and nuclear morphology," *Opt. Express* **5**, 302–317 (1999).
8. A. Kienle, L. Lielge, M. S. Patterson, R. Hibst, R. Steiner, and B. C. Wilson, "Spatially resolved absolute diffuse reflectance measurements for noninvasive determination of the optical scattering and absorption coefficients of biological tissue," *Appl. Opt.* **35**, 2304–2314 (1996).
9. A. Kienle, M. S. Patterson, N. Dögnitz, R. Bays, G. Wagneiers, and H. van den Bergh, "Noninvasive determination of the optical properties of two-layered turbid media," *Appl. Opt.* **37**, 779–791 (1998).
10. G. Alexandrakis, T. J. Farrell, and M. S. Patterson, "Accuracy of the diffusion approximation in determining the optical properties of a two-layer turbid medium," *Appl. Opt.* **37**, 7401–7410 (1998).
11. T. H. Pham, T. Spott, L. O. Svaasand, and B. J. Tromberg, "Quantifying the properties of two-layer turbid media with frequency domain diffuse reflectance," *Appl. Opt.* **39**, 4733–4745 (2000).
12. A. Pifferi, A. Torricelli, P. Taroni, and R. Cubeddu, "Reconstruction of absorber concentrations in a two-layer structure by use of multi-distance time-resolved reflectance spectroscopy," *Opt. Lett.* **26**(24), 1963–1965 (2001).
13. S. K. Chang, D. Arifler, R. Drezek, M. Follen, and R. Richards-Kortum, "Analytical model to describe fluorescence spectra of normal and preneoplastic epithelial tissue: comparison with Monte Carlo simulations and clinical measurements," *J. Biomed. Opt.* **9**, 511–522 (2004).
14. L. Wang and S. L. Jacques, "Hybrid model of Monte Carlo simulation and diffusion theory for light reflectance by turbid media," *J. Opt. Soc. Am. A* **10**, 1746–1752 (1993).
15. G. Alexandrakis, T. J. Farrell, and M. S. Patterson, "Monte Carlo diffusion hybrid model for photon migration in a two-layer turbid medium in the frequency domain," *Appl. Opt.* **39**, 2235–2244 (2000).
16. B. B. Das, K. M. Yoo, and R. R. Alfano, "Ultrafast time-gated imaging in thick tissues: a step toward optical mammography," *Opt. Lett.* **18**(13), 1092–1094 (1993).
17. S. G. Demos and R. R. Alfano, "Optical polarization imaging," *Appl. Opt.* **36**(1), 150–155 (1997).
18. S. L. Jacques, J. R. Roman, and K. Lee, "Imaging superficial tissues with polarized light," *Lasers Surg. Med.* **26**, 119–129 (2000).
19. A. D. Kim, "Transport theory for light propagation in biological tissue," *J. Opt. Soc. Am. A* **21**, 797–803 (2004).
20. A. D. Kim, "A boundary integral method to compute Green's functions for the radiative transport equation," *Waves in Random Media* (in press).
21. E. J. Hinch, *Perturbation Methods*, Cambridge University Press, New York (1991).
22. M. A. Franceschini, S. Fantini, L. A. Paulescu, J. S. Maier, and E. Gratto, "Influence of a superficial layer in the quantitative spectroscopic study of strongly scattering media," *Appl. Opt.* **37**, 7447–7458 (1998).
23. A. D. Kim and M. Moscoso, "Beam propagation in sharply peaked forward scattering media," *J. Opt. Soc. Am. A* **21**, 797–803 (2004).